

# IMAGING METHODOLOGY FOR DENSITY DISTRIBUTION AND CARBONATION DEPTH OF CONCRETE SPECIMENS USING HYPERSPECTRAL ANALYSIS

Yuzhe WANG\*<sup>1</sup>, Ryoma KITAGAKI\*<sup>2</sup> and Dayoung OH\*<sup>3</sup>

The current state of experiments regarding the ability to study hyperspectral images for the identification of the depth of carbonation on concrete surfaces is summarized in this paper. A series of concrete samples of different types were subjected to carbonation acceleration simultaneously. These samples were then photographed using a hyperspectral camera to obtain their hyperspectral data and analyzed. Based on the current study, carbonation fronts, areas of carbonation with varying degrees of body, and various aggregates in the concrete can be observed from the hyperspectral data.

Keywords: hyperspectral imaging, carbonation depth, density distribution, cross-section, NIR spectra

## 1. INTRODUCTION

Carbon sequestration has become an important issue in the field of construction in the face of increasing global warming[1]. The purpose of this experiment is to explore the possibility of using a hyperspectral camera and its data to analyze the depth of carbonation on concrete surfaces, with the aim of non-destructive carbonation detection in buildings. Since the inception of the experiment, we have conducted several experiments and combined them with programming languages such as python, and have reached the milestone of producing images that can differentiate the carbonated areas of the concrete surface from those that are uncarbonated.

## 2. TEST PROGRAMS

### 2.1 Materials

#### (1) Powdery reagent

The specifications and manufacturers of calcium carbonate powder and calcium hydroxide powder used in the experiments described in 2.1 are shown in Table 1.

#### (2) Concrete specimens

Table 2 shows the mixture proportions of each concrete of the uncarbonized specimens described in 2.4. The mixture proportions are identical except that the coarse aggregates are limestone or hard sandstone, respectively. The specimens were cast in cylindrical molds 100 mm in diameter and 200 mm in height and sealed and cured for 28 days. One specimen of each type of concrete was used as an accelerated carbonation specimen. To intrude carbon dioxide only in the vertical direction, taped with aluminum tape with butyl rubber, leaving only the upper surface. They were placed in an accelerated carbonation container at 20°C, 60% relative humidity, and 5% carbon dioxide concentration for 60 days of accelerated carbonation in a wet-dry cycling

device as shown in Figure 1. One side of the bottles filled with water and desiccant is connected to a pump, and the other is connected to the sample container. By setting a switch, when dry air is needed, air passed through a desiccant is introduced into the sample container, and when moist air is needed, air passed through water is introduced into the sample container.

This device can circulate from 20% RH to 80% RH once a day, which can effectively accelerate the

**Table.1 Specification of materials**

Powder	manufacturer	Particle size	Product Grade
Calcium carbonate	Kanto Chemical	10 μ m	category A
Calcium hydroxide	Kanto Chemical	10 μ m	category A

**Table.2 Amount of material required per 1m<sup>3</sup>**

	Cement (kg)	Water (kg)	Coarse Aggregate(kg)	Fine Aggregate(kg)
Limestone concrete	327	196	942	931
Sandstone concrete	327	196	920	917

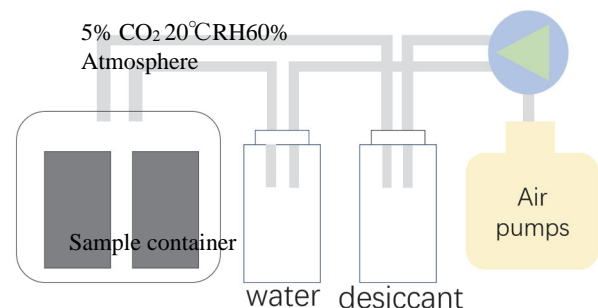


**Fig. 1 Schematic diagram of wet/dry circulation device for accelerated carbonation**

\*1 Graduate School of Engineering, Hokkaido Univ., JCI Student Member

\*2 Prof., Graduate School of Engineering, Hokkaido Univ., Dr.E., JCI Member

\*3 Assistant Prof., Graduate School of Engineering, Hokkaido Univ., Dr.E., JCI Member

carbonation of the samples. The same number of specimens were left in the outdoor environment as a control group. The coarse aggregate for two accelerated carbonized samples were limestone and sandstone, respectively, which was the same as for the non-accelerated carbonized samples.

## 2.2 Hyperspectral camera and analytical method

### (1) Hyperspectral camera performance and imaging conditions

The hyperspectral camera was a SWIR-640 camera manufactured by Hypspx. It can provide hyperspectral data for targets in the range 960-2500nm. The shooting distance was 30 cm, the illuminator was two halogen lamps, and the illumination level of 3000 lx ensured that enough infrared light entered the lens.

In addition, all of the following test objects were measured under essentially the same measurement conditions. The test rig is shown in Figure 2.

### (2) Hyperspectral data acquisition methods

Using the software spectron, produced by Resonon, it is possible to select pixel points or regions based on color images and obtain their hyperspectral data, as shown in Figure 3. The raw data obtained is noisy and needs to be smoothed by noise reduction before analysis.

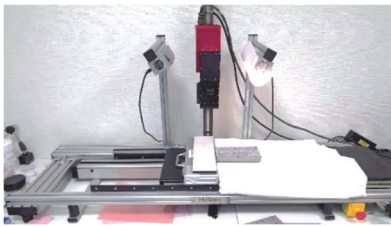


Fig.2 Hyperspectral photography test site

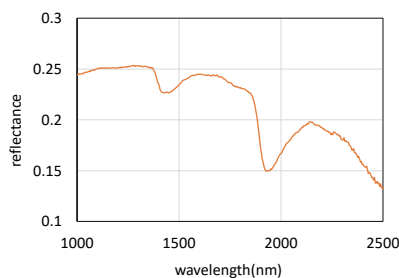


Fig.3 Example of a hyperspectral data plot

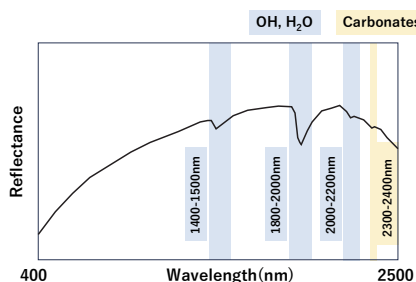


Fig.4 Spectral attribution of clay minerals based on literature review

### (3) Spectral attribution from data of hyperspectral images

Hyperspectral cameras are commonly used on

board aircraft and satellites to study the distribution of minerals and plants on the earth's surface. In laboratory analysis, wavelength 400 to 2500 nm is in the visible to near-infrared region, and attribution can be evaluated from existing NIR spectroscopy data.

Related components to our study can be interpreted in using existing studies on the spectra with clay minerals exposed on the ground surface, calcium carbonate, moisture, organic content, and PH. However, attributions that can be applied to concrete should be carefully conducted due to the complexity of the mixture composition. Specifically, clay minerals have OH absorption peaks around 1400-1500, 1800-2000, and 2000-2200 nm, and as their content increases, they absorb electromagnetic waves widely over the entire 400-2000 nm range, which is characterized by a lowering of the baseline of the reflectance spectrum[2]. Calcium carbonate has no large absorption peak at 400-2000 nm and a small absorption peak at 2200-2300 nm[2]. The attributions are summarized in Figure 4.

On the other hand, since calcium hydroxide is not often found on the ground surface in nature, there are few research reports on the spectral features of calcium hydroxide. In addition, in the case of imaging using a multispectral camera, the images are taken in an open system. Since the amount of energy from reflected light tends to vary, a spectrum is obtained in which small peaks are added to a large baseline and noises. The large baseline is difficult to attribute because it is caused by various minerals that have high reflectance over the entire wavelength range of the measurement. Generally, in the field of image analysis of aerial photographs and satellite images, the continuum removal method (shortly CR method) is used as a preprocessing method to extract small characteristic spectra from spectral data obtained by a multispectral camera[3].

CR method specifies absorption peaks expected from the data and removes manually large baselines by literature. However, since the baseline also make fluctuations with changes in the composition of the sample, there are many studies that interpret the slope of the baseline obtained by the CR method for using it qualitatively[4]

## 2.3 Mixed powder measurement

### (1) Spectral analysis of each powder

The calcium hydroxide and calcium carbonate reagents given in Section 2.1 were placed on white paper as shown in Figure 5. Measurements were made using a hyperspectral camera under the imaging conditions given in Section 2.2 to obtain spectral images.

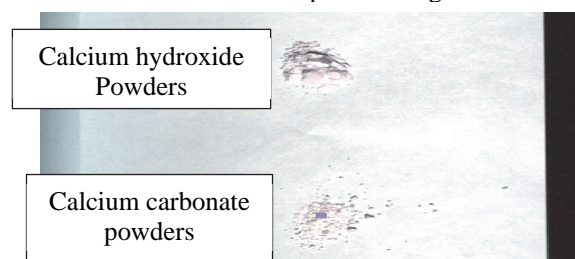


Fig.5 Calcium Carbonate Powder & Calcium Hydroxide Powder

(2) Mixed powder measurement

Calcium carbonate powder and calcium hydroxide powder given in 2.1 were mixed in different proportions and photographed in the environment described in 2.2. The content of calcium carbonate powder was increased in 10% increments from 0% to 100%, while the rest of the mixture consisted entirely of calcium hydroxide. The mixed powders are placed as in Figure 6.

2.4 Evaluation of carbonation specimens of two types of coarse aggregate

The two uncarbonized and carbonized specimens described in Section 2.1 were cut axially along the center of the cylinder with a wet blade and then quickly placed in a vacuum desiccator at room temperature for at least one month to dry the surface.

A portion of the cut surface was then covered, exposing only the edge portion on one side, and this portion was stained with phenolphthalein solution, followed by hyperspectral camera photography.

3. Discussion

3.1 Spectral analysis of each powder

Hyperspectral data for the calcium hydroxide and calcium carbonate reagents are shown in Figure 7a. Calcium hydroxide is detected with a distinct negative peak at 1400 nm. There is a small positive peak in the 2350-2450 range for calcium carbonate and an absorbance peak for calcium hydroxide as shown in Figure 7b. This indicates that this region can be used for selecting calcium carbonate and calcium hydroxide.

3.2 Multispectral data of mixed powder

As shown in Figure 8a and b, the peak absorbance near 2400 nm decreases as the mixing ratio of calcium carbonate increases. According to Figure 8cd the peak absorbance near the 1450 nm wavelength also decreases when the mixing ratio of calcium carbonate exceeds

50%, both of which change rapidly. On the contrary, when the mixing proportion of calcium hydroxide increases, the peaks at both locations tend to increase.

3.3 Carbonation specimen evaluation of two types of coarse aggregate

(1) Density and carbonation depth imaging based on reagent attribution strategy

For generating color images, we use the spectral library in python to read the hyperspectral data of each pixel point and then calculate it using a designed formula so that each pixel point gets a corresponding value and a dataset is generated. Matplotlib was then used to obtain the color images.

Based on the results of Sections 3.1 and 3.2 with reference to Figure 9 considering that the depth of the peak at 1400-1450 nm is related to the concentration of calcium hydroxide, the calcium hydroxide concentration index  $V_{ch}$ , was prepared and utilized for imaging as shown in Fig. 10b with the following equation.

In general, the reflectance across the spectrum becomes smaller when the clay mineral density is high, so the smaller the reflectance  $R_{1350}$  at 1350 nm, the higher the clay mineral content, which was utilized to perform the imaging as shown in Figure 10c. The results of the imaging using  $R_{1350}$  are shown in Figure 10b. The results of the imaging using  $R_{1350}$  are as follows. We also attempted to multiply  $R_{1350}$  by  $V_{ch}$ , which highlights regions of high calcium hydroxide content and low density. Therefore, to verify the possibility of observing transition zones, we also imaged  $V_{ch} \times R_{1350}$ . The results are shown in Figure 10d.

In the  $V_{ch}$  image, it can be seen that the areas outside the aggregate are essentially blue in color with different depths, corresponding to the presence of calcium hydroxide in the cement paste, with the deeper the blue color the higher the calcium hydroxide concentration. In the  $R_{1350}$  image, the aggregate is

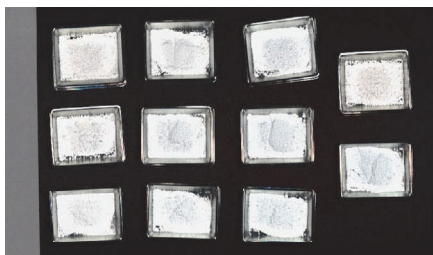


Fig.6(a) Calcium carbonate powder mixed with calcium hydroxide powder

10%CH +90%CC	40%CH +60%CC	70%CH +30%CC	100%CH
20%CH +80%CC	50%CH +50%CC	80%CH +20%CC	100%CC
30%CH +70%CC	60%CH +40%CC	90%CH +10%CC	

Fig.6(b) Various mixing ratios of powders and their locations

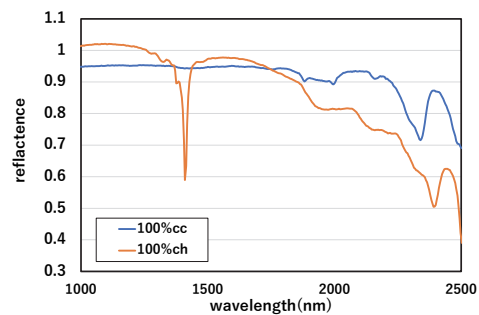


Fig.7(a)

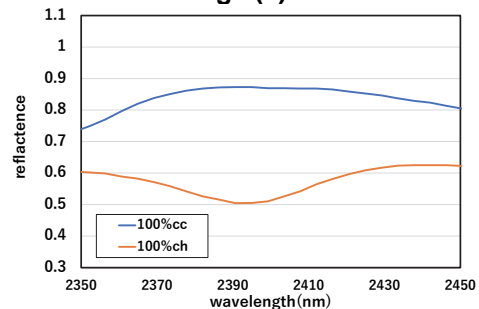


Fig.7(b)

reddish in color, the dense regions are highlighted, and the cement paste and aggregate are clearly separated and shown. Furthermore, in the Vch x R1350 image, the aggregate density and calcium hydroxide density are clearly separated as vch and r1350 increase and decrease. On the other hand, the calcium hydroxide concentration in each region was not actually verified, so only qualitative judgments could be made. In addition, the depth of carbonation could not be determined from this set of images.

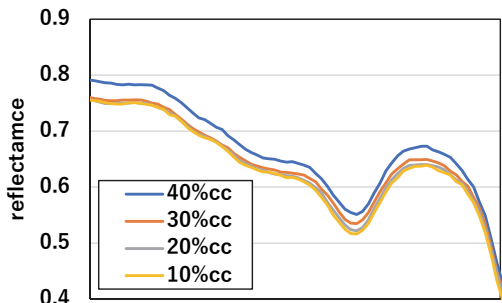


Fig.8(a)

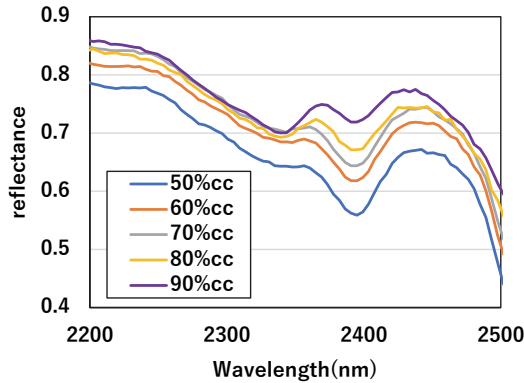


Fig.8(b)

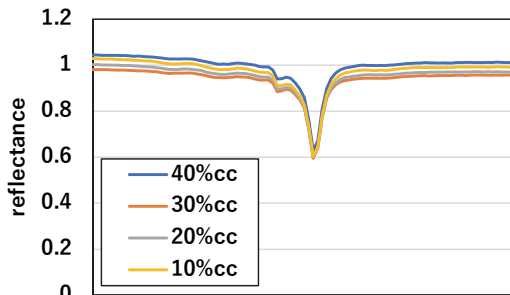


Fig.8(c)

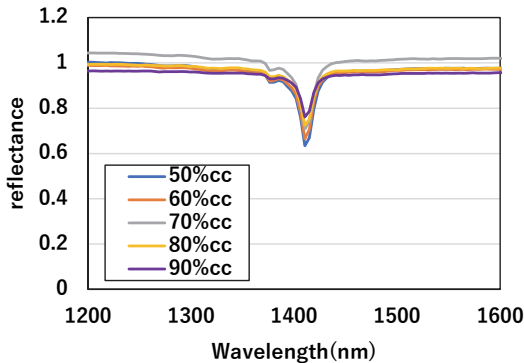


Fig.8(d)

## (2) Accelerated Carbonation Depth Imaging of Carbonated and Uncarbonated Specimens

Due to the difficulty of assessing the carbonation depth using the method presented in (1), a statistical assessment of the baseline change with increasing calcium carbonate was considered.

Five points were randomly selected at 2, 7, 12 and 17 mm depth from the surface of the accelerated carbonated specimens and the hyperspectral data were further normalized. For each depth, the value of 1000 nm reflectance spectra was taken as 1 to normalize the five sets of data. For each set of data 1967 nm was made the baseline and used as it.

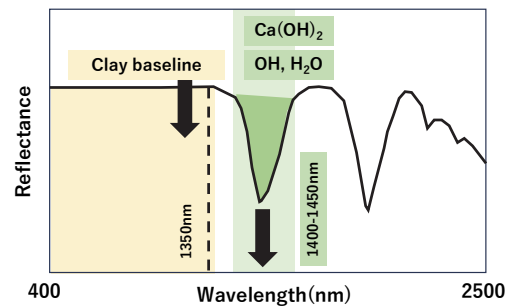


Fig.9 Spectra used for attribution and evaluation in concrete specimens

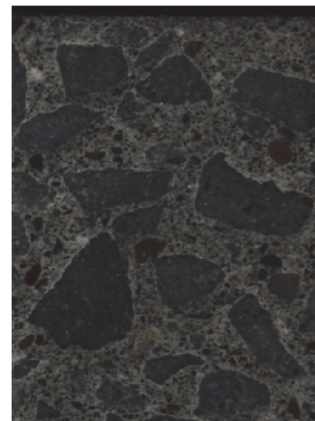


Fig.10(a) A rectangular area 5cm by 8cm on the concrete surface

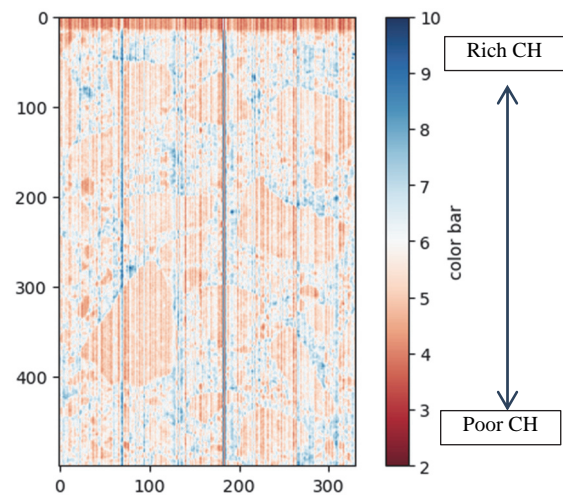
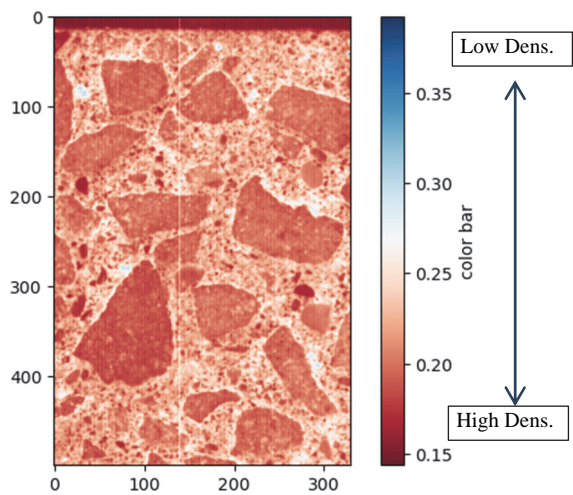
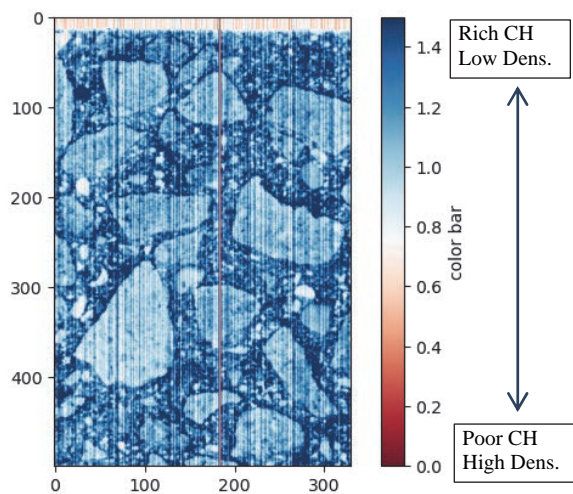


Fig.10(b) Image the Vch data



**Fig.10(c) Image the R1350 data**



**Fig.10(d) Image the Vch x R1350**

According to Figure 11, it can be seen that the slope of the baseline gradually increases with increasing depth. This was not the case with the same treatment for the samples that were not carbonated, and the slopes were larger except at 2 mm. According to the results of this study, the higher the degree of carbonation, the higher the rate of change. The baseline tends to slope to the right in areas with a higher degree of carbonation. So we make the image with the tilt rate of the baseline.

Figure 12 below shows images of hard sandstone coarse aggregate and limestone coarse aggregate specimens. The box on the left is the phenolphthalein stained area. It can be seen that in both accelerated carbonation samples, the larger blue area observed from the upper surface is consistent with the carbonation area of the accelerated carbonation samples. In contrast, in the sample placed in a normal environment, only blue areas are observed at the surface, which is also consistent with the carbonation of the sample. This result provides some indication of the depth of carbonation. It is worth noting that some of the coarse aggregates also appear blue in color because of the large amount of calcium carbonate in the hard sand and gravel.

**4. Conclusion**

After a series of experiments, it is now possible to determine that it is possible to distinguish the various aggregates in concrete, the cement paste, by means of hyperspectral data. It is also possible to distinguish between areas where carbonation has occurred and areas where carbonation has not occurred. From the color of carbonated areas, it can be seen that the depth of the color varies from the surface to the inside, which is in

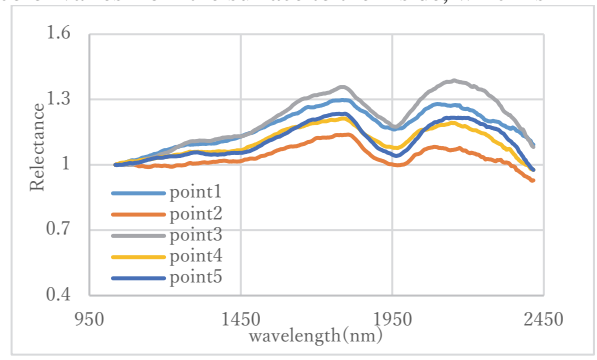


**Fig.11(a) Normalized spectral data at 2 mm depth**

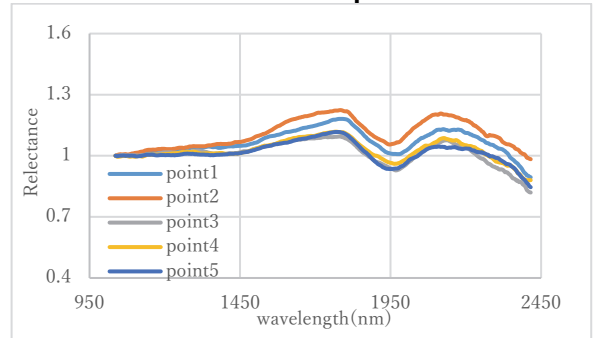


**Fig.11(b) Normalized spectral data at 7 mm depth**

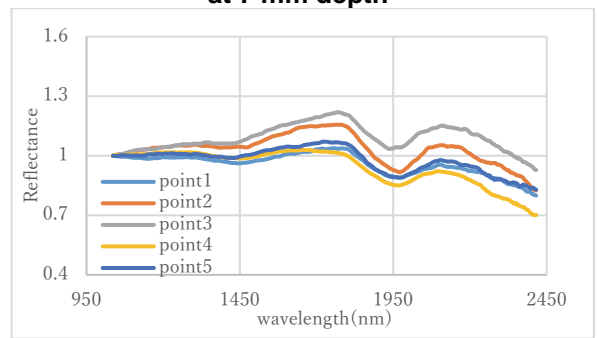


**Fig.11(c) Normalized spectral data at 12 mm depth**

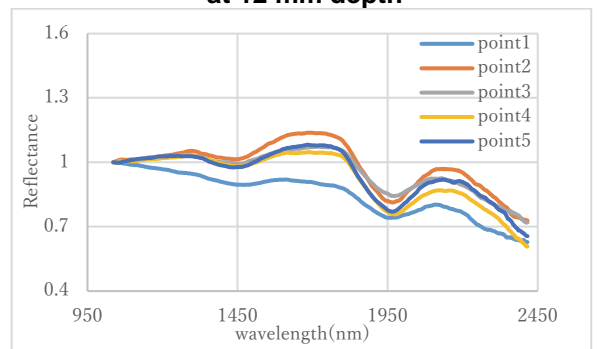


**Fig.11(d) Normalized spectral data at 17 mm depth**

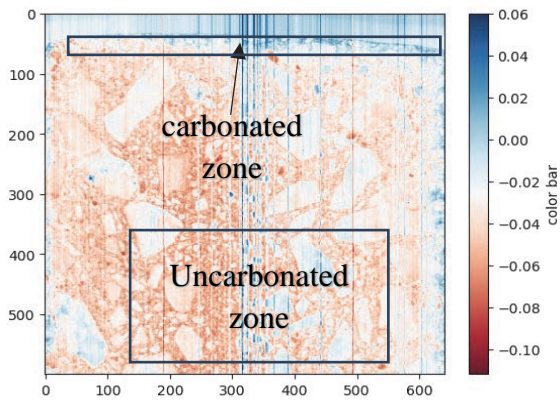


**Fig.12(a) Limestone concrete surfaces without accelerated carbonation**

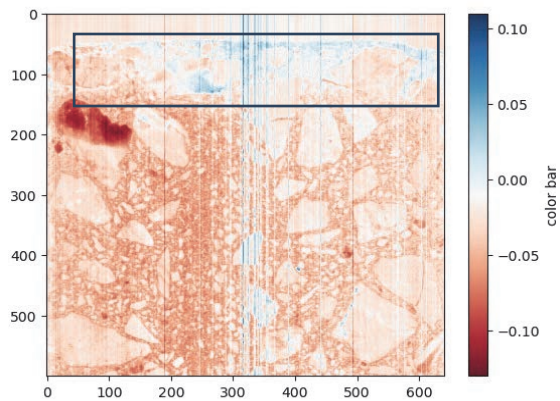


**Fig.12(b) Limestone concrete surfaces with accelerated carbonation**

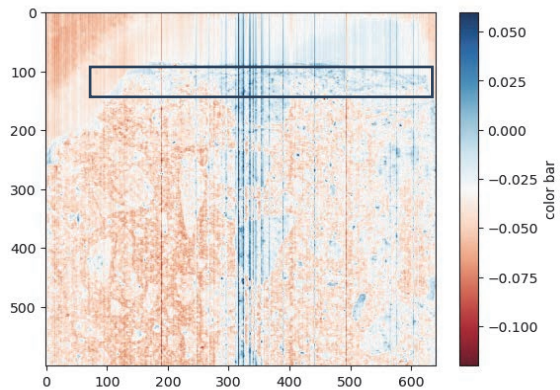


**Fig.12(c) Sandstone concrete surfaces without accelerated carbonation**

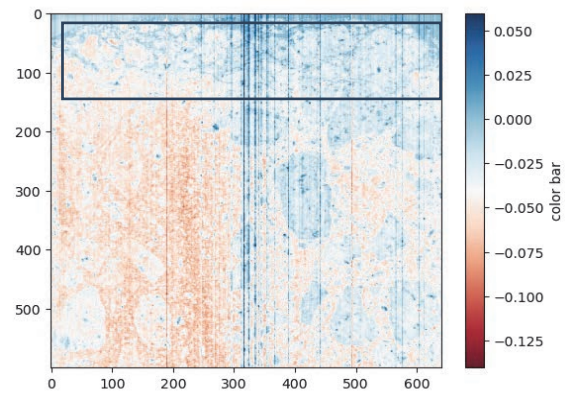


**Fig.12(d) Sandstone concrete surfaces with accelerated carbonation**

line with the law that the degree of carbonation becomes lighter and lighter from the surface to the inside. However, the current experiments are not able to determine the specific carbonation degree of these areas and the content of calcium carbonate in the carbonated areas. It may be possible to derive the specific calcium carbonate content by comparing the normalized hyperspectral data of the mixed powder with that of the concrete surface, but a series of experiments are needed to verify this.

#### ACKNOWLEDGEMENT

This study was based on the results obtained from a project (JPNP21023) commissioned by the New Energy and Industrial Technology Development Organization (NEDO). The authors thank NEDO for its support.

#### REFERENCES

- [1] Churkina, G. et.al.:Buildings as a global carbon sink. *Nat Sustain* 3, 269–276 (2020).
- [2] Salman Naimi. et.al.:Quantification of some intrinsic soil properties using proximal sensing in arid lands: Application of Vis-NIR, MIR, and pXRF spectroscopy, *Geoderma Regional*, Volume 28, 2022
- [3] Asgari, N. et.al.:Carbonates and organic matter in soils characterized by reflected energy from 350–25000 nm wavelength. *J. Mt. Sci.* 17, 1636–1651, 2020
- [4] Philippe Lagacherie et.al.:Estimation of soil clay and calcium carbonate using laboratory, field and airborne hyperspectral measurements, *Remote Sensing of Environment*, Volume 112, Issue 3, Pages 825-835, 2008